

Supplementary Information

Linking Fundamentals and Devices: Evaluating Low Pt Ag Nanocatalysts in Three-Electrode Systems and Operating Glycerol AEM Electrolyzers

Carlos C. Lima^{†,a,b}, Ana Luz Tupa Quispe^{†,a,b}, Victor Y. Yukuhiro^{a,b}, Cléo T. G. V. M. T. Pires^{a,b, δ}, Ana B. S. Silva^{a,c}, Richard Landers^d, Patrick B.S. de Figueiredo^e, Roberto B. de Lima^e, Marco A. Z. Arruda^{a,c}, Keyla Teixeira Santos^{a,b*}, José J. Linares,^{f*} and Pablo S. Fernández^{a,b*}

^a Institute of Chemistry, State University of Campinas (UNICAMP), Campinas SP, 13083-970, Brazil.

^b Center for Innovation on New Energies (CINE), Campinas SP, 13083-841, Brazil.

^c Spectrometry, Sample Preparation and Mechanization Group, Institute of Chemistry, State University of Campinas (UNICAMP), Campinas SP, 13083-970, Brazil.

^d Institute of Physics Gleb Wataghin, State University of Campinas (UNICAMP), Campinas SP, 13083-859, Brazil.

^e Chemistry Department, Exact Science and Technology Center, Federal University of Maranhão, São Luís 65080-805, Brazil.

^f Institute of Chemistry, University of Brasília, Campus Universitário Darcy Ribeiro, Brasília 70910-900, Brazil.

^δ Current address: Department of Chemistry “Giacomo Ciamician” Alma Mater Studiorum University of Bologna, Via P. Gobetti 85, Bologna 40129, Italy.

[†]These authors contributed equally to this work.

* Corresponding authors: pablosf@unicamp.br (PSF), joselinares@unb.br (J JL), keylats@unicamp.br (KTS).

Table of Contents

Table S1. Mass quantification of Pt in Ag-based materials by ICP and XPS	S3
Figure S1. High-resolution XPS spectra of Pt 4f and Ag 3d regions	S4
Figure S2. Differential thermal and thermogravimetric analysis (DTG/TGA) curves	S4
Discussion of ICP and TGA Analysis Procedures Sample digestion challenges Nitric acid digestion method Reproducibility and comparison of Metal/Carbon ratios	S4
Figure S3. Chromatograms of Pt(x%)Ag/C and Pt/C samples	S6
Figure S4. HPLC calibration curves for glycerate, glycolate, lactate, and formate	S7
Figure S5. Cyclic voltammograms for Pt(0.3%)Ag/C, Pt/C, and Ag/C for ethanol electro-oxidation	S8
Supplementary Notes 1. Preparation of PtAg/C catalyst employed in electrolyzer tests	S8
Table S2. Mass quantification of Pt in Ag-based material by ICP-OES	S9
Figure S6. XRD pattern and cyclic voltammograms of Ag/C, PtAg/C, and Pt/C catalysts	S9
Figure S7. Chromatograms during LSV in electrolyzer device	S10
Figure S8. Photographs illustrating the electrolyzer device assembly steps	S10
Figure S9. Cyclic voltammograms for Pt0.5Ag/C using different counter electrodes	S11
Figure S10. Products selectivity at 0.9 V vs RHE for GEOR on various catalysts	S11
Figure S11. Linear sweep voltammetry and chromatograms for Ag/C catalyst	S12
References	S12

Table S1. Mass quantification of Pt in Ag-based by ICP and XPS

	ICP	XPS
Sample	Pt/(Pt+Ag)	
	mass (%)	mass (%)
Pt(0.3%)Ag/C	0.3±0.01	9.1
Pt(0.5%)Ag/C	0.5±0.05	37
Pt(6.9%)Ag/C	6.9±0.5	62

Table S1 allows us to compare mass percentage values of the data obtained by ICP and XPS. The much higher Pt percentages obtained by XPS are a clear indication of a successful application of the galvanic replacement approach, whose main aim was to concentrate the noble metal at the surface of the particles.

XPS analysis was used to understand better the sample's surface chemical composition, which provides information to a depth of about ~5 nm.¹ Pt 4f spectra are shown in Figure S1a. Curves deconvolution and fit lead to two doublets. According to their binding energy, two are assigned to Pt²⁺ and two to Pt⁰ species. It was observed that AgCl in the sample is sensitive to the XPS X-ray source, leading to a change in the spectrum with time. This sensitivity of AgCl has already been observed in other works.²⁻⁴ Due to this phenomenon, Ag⁺ was not observed, and the stable spectrum at high resolution shows only Ag⁰ (Figure 2b).

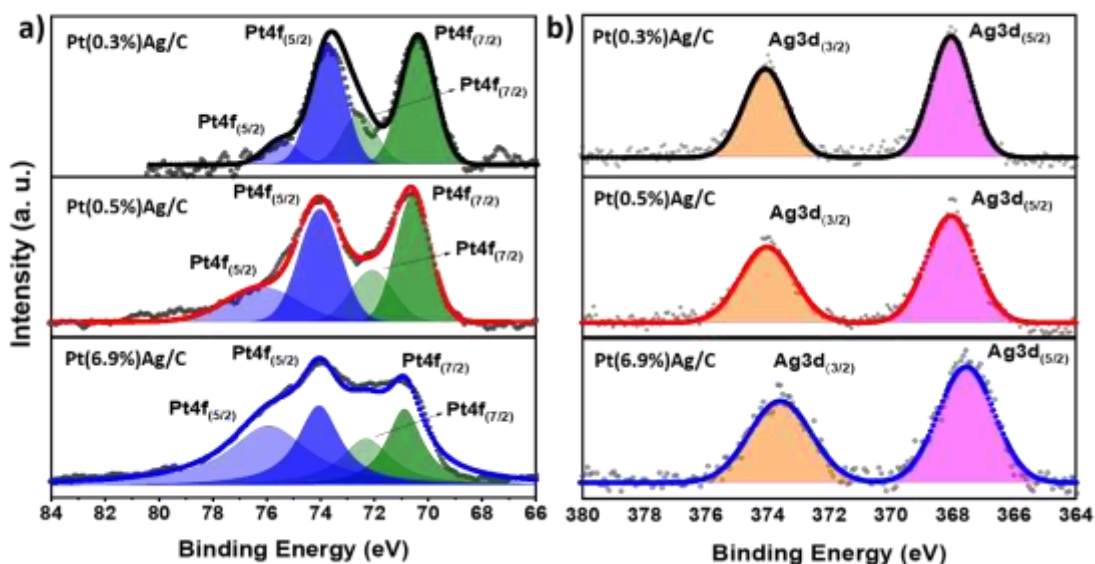


Figure S1. High-resolution XPS spectra of (a) Pt 4f and (b) Ag 3d regions for Pt(0.3)Ag/C, Pt(0.5)Ag/C, and Pt(6.9)Ag/C samples.

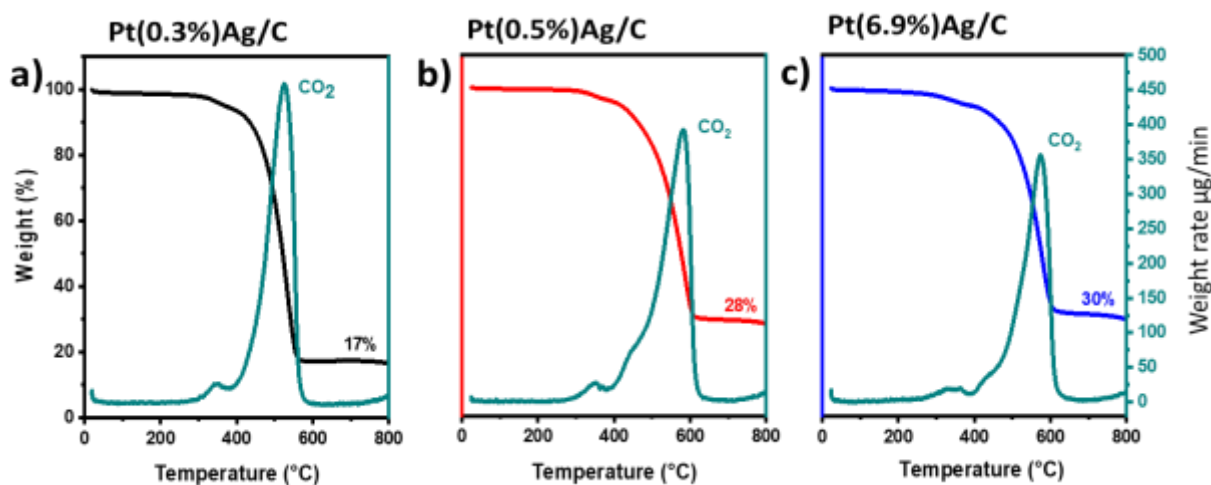


Figure S2. – Differential thermal and thermogravimetric analysis (DTG/TGA) curves of a) Pt(0.3%)Ag/C, b) Pt(0.5%)Ag/C and c) Pt(6.9%)Ag/C powder. Instrumental error is $\leq 0.1\%$

All TGA curves start without any significant weight loss due to the low amount of physically adsorbed water. Around 400°C, a sharp weight loss is observed due to carbon decomposition.⁵ After carbon oxidation, the corresponding residual metal mass values found were 17%, 28%, and 30% for Pt(0.3%)Ag/C, Pt(0.5%)Ag/C and Pt(6.9%)Ag/C, respectively. Through these values

obtained by the analysis of TGA and ICP, we determined numerical factors used in the current normalization for electrochemical experiments.

When using ICP for metal-supported nanoparticles, most samples are digested using *aqua regia*. However, in this case, the presence of Ag did not allow us to use this mixture of acids as Ag nanoparticles oxidize, forming Ag ions that precipitate as AgCl. Thus, we used concentrated nitric acid digestion as an alternative procedure. Unfortunately, this reactant is a much weaker oxidizing agent, making the procedure more laborious. Besides, the boiling nitric acid does not completely dissolve the carbon. Then, filtration is required before injection on both ICP-OES and ICP-MS (we used both methodologies to validate our results).

This weaker oxidation power obliged us to digest relatively small quantities of the catalysts (10mg). Therefore, as the materials are not perfectly homogeneous, with diverse metal particles dispersion on the carbon and different Pt covering on Ag particles, we got different Metal/Carbon ratios for different measurements with the same material. On the other hand, the dispersion in the Pt/Ag ratio was much smaller (see the slight average absolute deviation in Table S1). Therefore, we considered that the relative amount of metals in our sample was the only reliable value obtained with ICP with our digestion procedure, thus discarding the Metal/Carbon data, as this information was obtained through the TGA measurements.

Another important point to pay attention to is the difference in the Metal/Carbon content of the three catalysts. Fortunately, Pt(0.5%)Ag/C and Pt(6.9%)Ag/C have both approximately the same value, validating all the conclusions of this paper and explaining the much lower currents of Pt(0.3%)Ag/C in Figure 4.

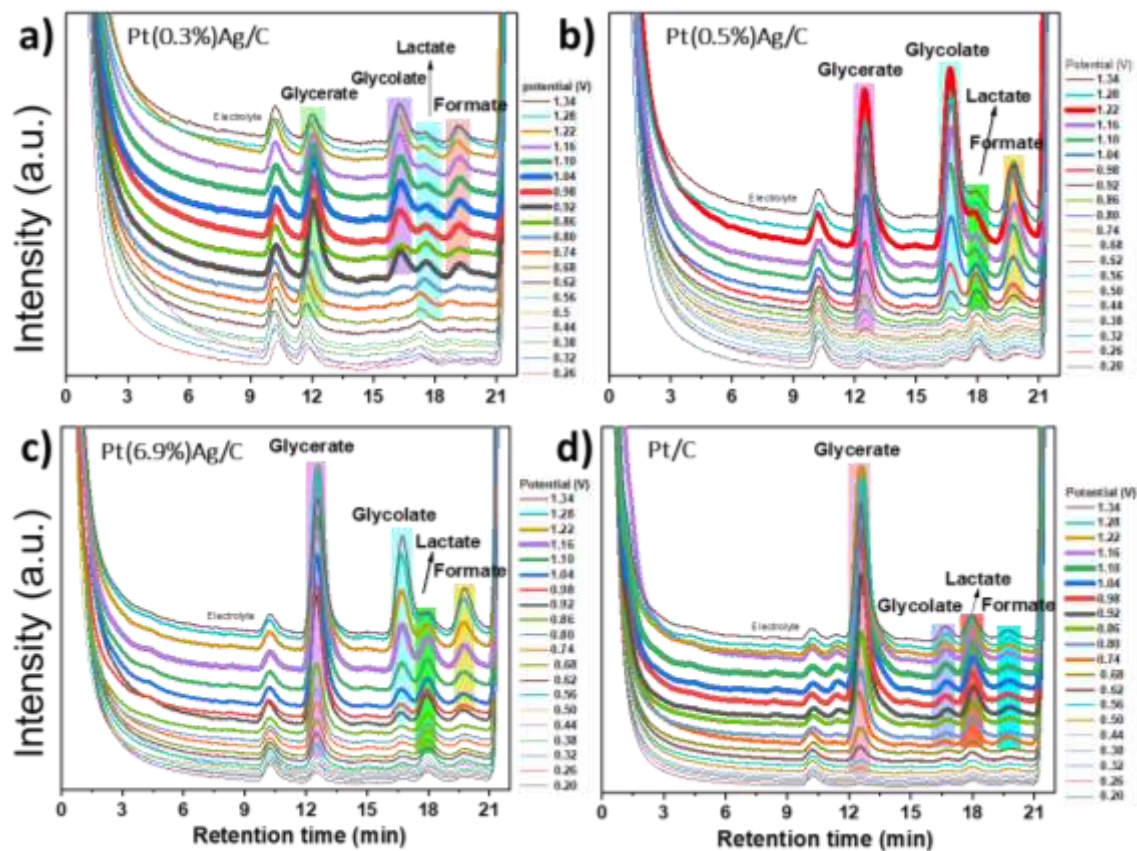


Figure S3. Chromatograms of the samples for a) Pt(0.3%)Ag/C b) Pt(0.5%)Ag/C c) Pt(6.9%)Ag/C d) Pt/C. Obtained potentials during linear voltammetry in the 0.2 – 1.35V range, scan rate 1.0 $\text{mV}\cdot\text{s}^{-1}$ at $0.5 \text{ mol}\cdot\text{L}^{-1}$ NaOH and $1.0 \text{ mol}\cdot\text{L}^{-1}$ GIOH.

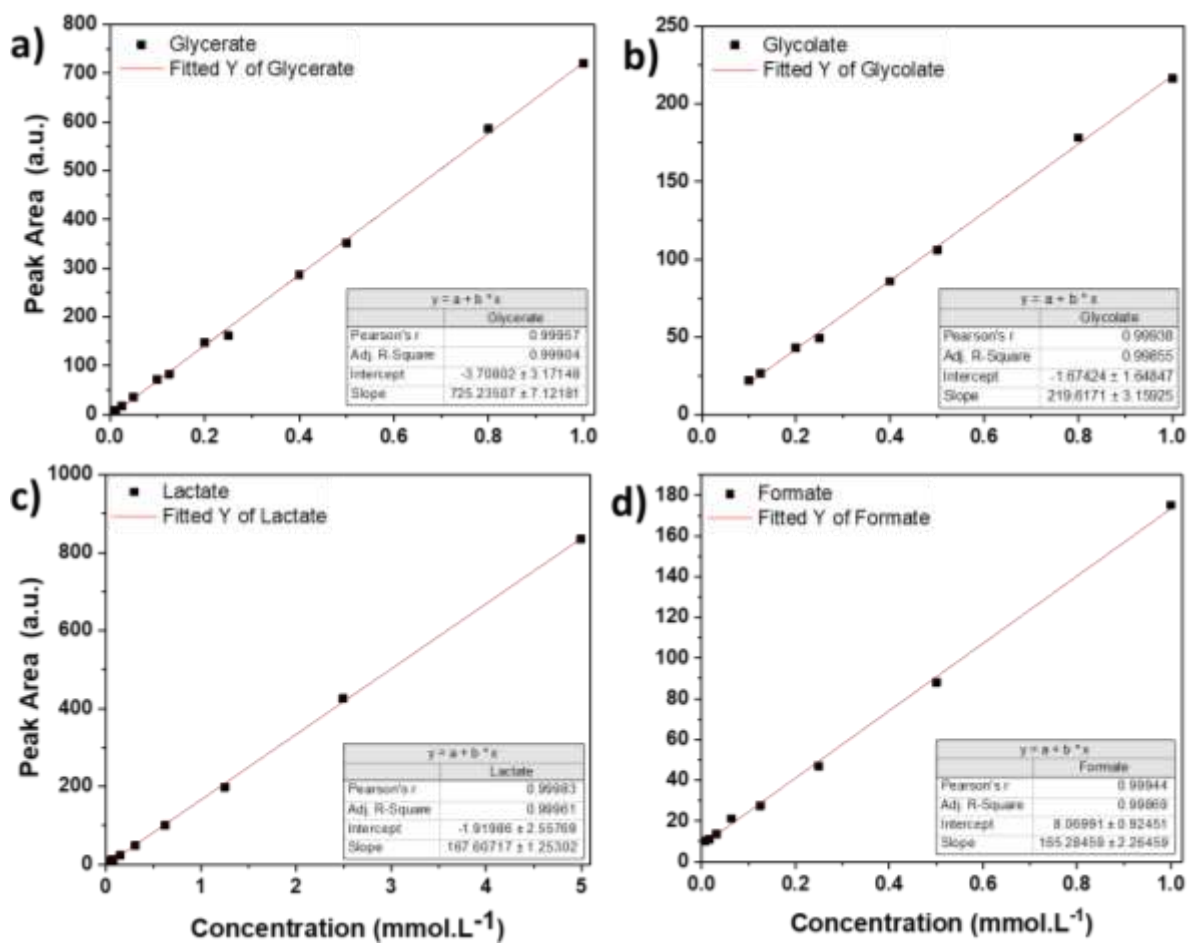


Figure S4. – HPLC calibration curves for (a) glycerate, (b) glycolate, (c) lactate and (d) formate.

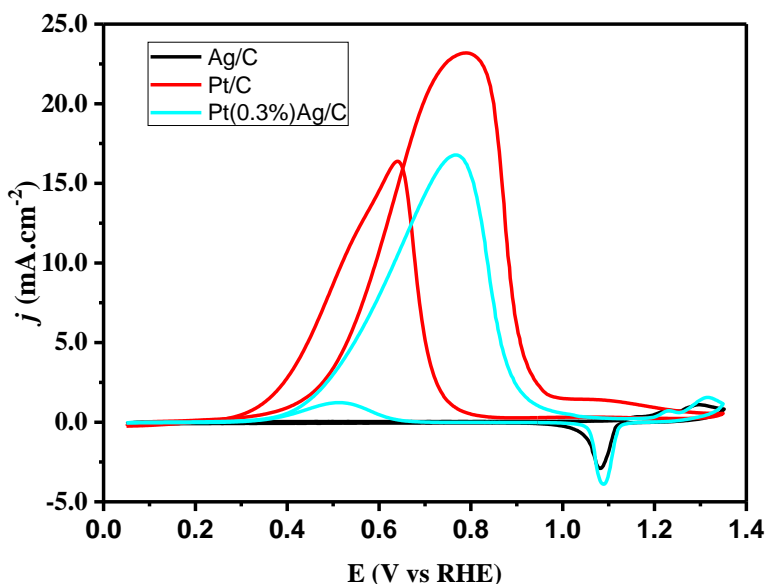


Figure S5. Cyclic voltammograms ($20 \text{ mV}\cdot\text{s}^{-1}$) obtained in $0.5 \text{ mol}\cdot\text{L}^{-1}$ NaOH and $1.0 \text{ mol}\cdot\text{L}^{-1}$ ethanol solution normalized by geometric area for Pt(0.3%)Ag/C, Pt/C and Ag/C. Scan 6.

Supplementary Notes 1

The PtAg/C catalyst employed in the electrolyzer tests was prepared according to the procedure described in Ref. ⁶. A solution of silver nitrate (AgNO_3 , 20 mM, Sigma-Aldrich®) was added to a boiling mixture of trisodium citrate (40 mM) and ultrapure water. The mixture was maintained under reflux for 30 hours. $\text{H}_2\text{PtCl}_6\cdot 6\text{H}_2\text{O}$ was added to promote surface modification with platinum via galvanic replacement, achieving a nominal platinum content of 2.4% (mol/mol). Carbon Vulcan XC-72 (60 mg) was added, and the resulting dispersion was subjected to ultrasonication for 30 minutes. To facilitate the immobilization of the nanoparticles onto the carbon support, the suspension was stirred continuously for 12 hours. Subsequently, the solid was washed with ultrapure water, centrifuged, and then dried in a Petri dish at 65°C for 24 hours. The 2.4% Pt loading was not chosen arbitrarily but was optimized to yield a CV profile for GEOR similar to that observed for the Pt(0.5%)Ag/C catalyst discussed in the manuscript. Due to the difference in the particle size of this batch, the lower Pt content (0.5%) resulted in electrochemical behavior

closer to that of pure Ag. Therefore, a higher Pt content was necessary to achieve comparable catalytic features.

The obtained materials were submitted to ICP-OES analysis, as were the previous materials. Table S2 shows the obtained metal percentage.

Table S2. Mass quantification of Pt in Ag-based material by ICP-OES.

Metal	Average mass (mg)	Pt (%)
Pt	0.08 ±0.02	2.37±0.04
Ag	3.29±0.01	-

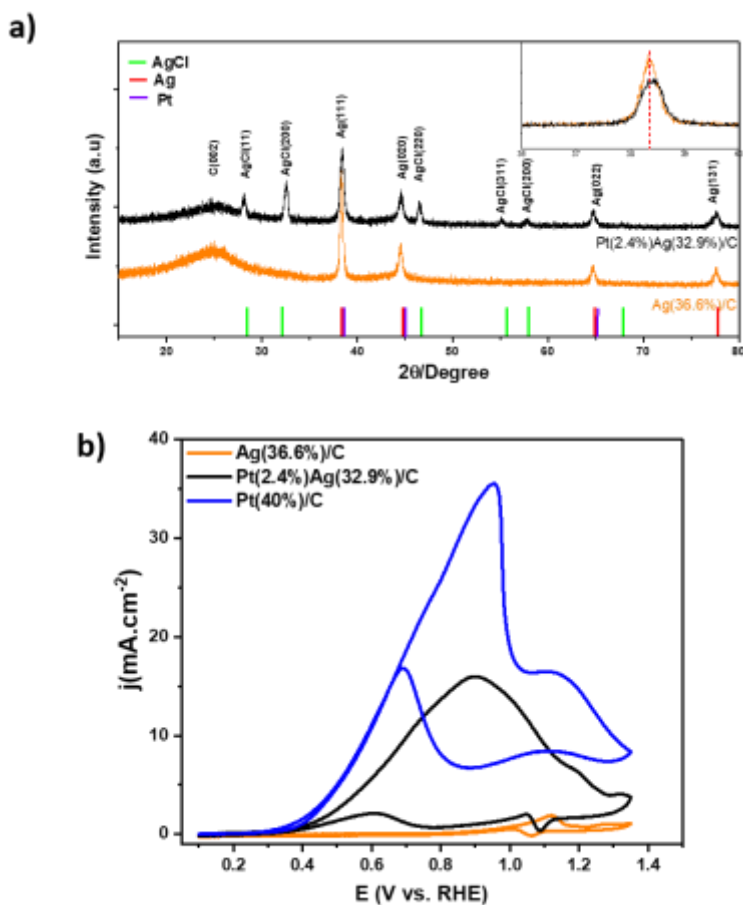


Figure S6: a) XRD pattern of Ag(36.6%)/C and Pt(2.4%)/Ag(32.9%)/C. Inset: Magnification of the (111) reflection of Ag to highlight peak position and possible shifts related to Pt deposition. b) CVs of Ag/C, PtAg/C and Pt/C catalysts in 0.5 mol.L⁻¹ NaOH and 1.0 mol.L⁻¹ GIOH at 20mV s⁻¹.

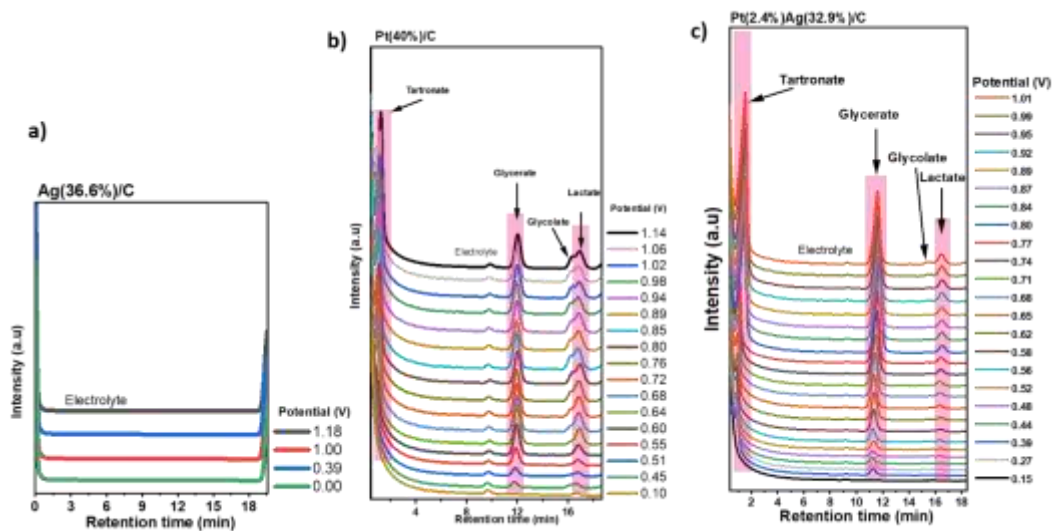


Figure S7. Chromatograms for a) Ag(36.6%)/C b) Pt(40%)/C c) Pt(2.4)Ag(32.9%)/C. Obtained during LSV in electrolyzer device each 2 minutes from 0.1 to 1.1V. Scan rate 0.1 mV.s⁻¹

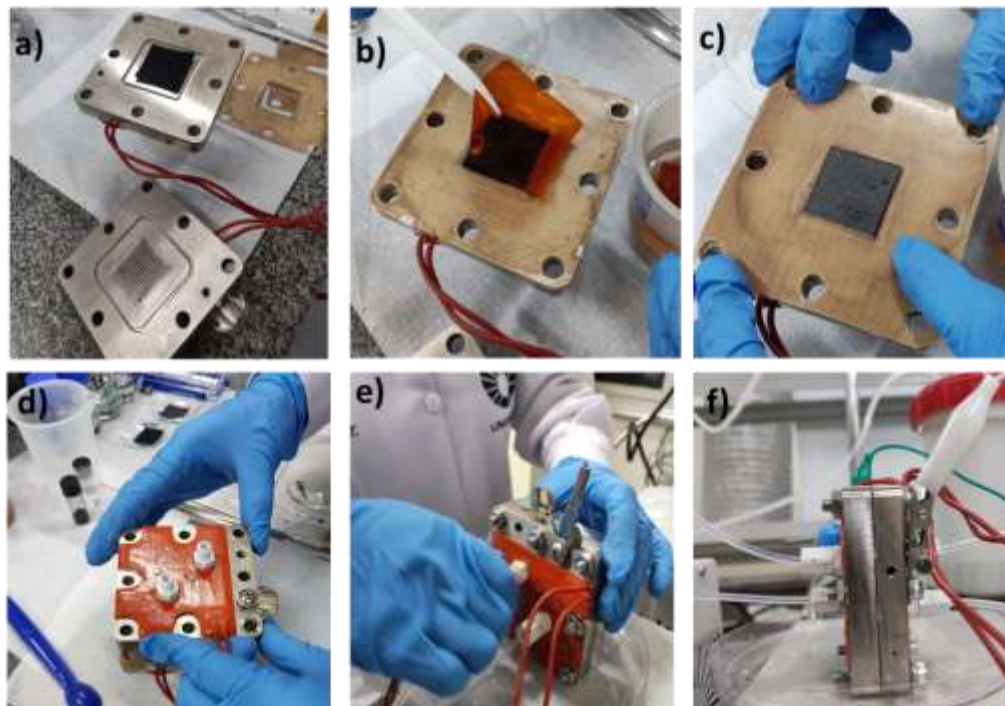


Figure S8. Photographs illustrating the assembly steps of the electrolyzer device. (a) Positioning of the anode catalyst layer onto the serpentine-patterned conductor plate. (b) Placement of the PTFE glass fiber fabric followed by the PBI membrane on top of the anode. (c) Placement of the cathode catalyst layer over the PBI membrane and addition of another PTFE glass fiber layer to insulate the plates. (d) Positioning of the cathode conductor plate over the assembled layers. (e) Tightening and securing the complete electrolyzer assembly. (f) Final assembly with connection of fluid tubes and electrical wiring for device operation.

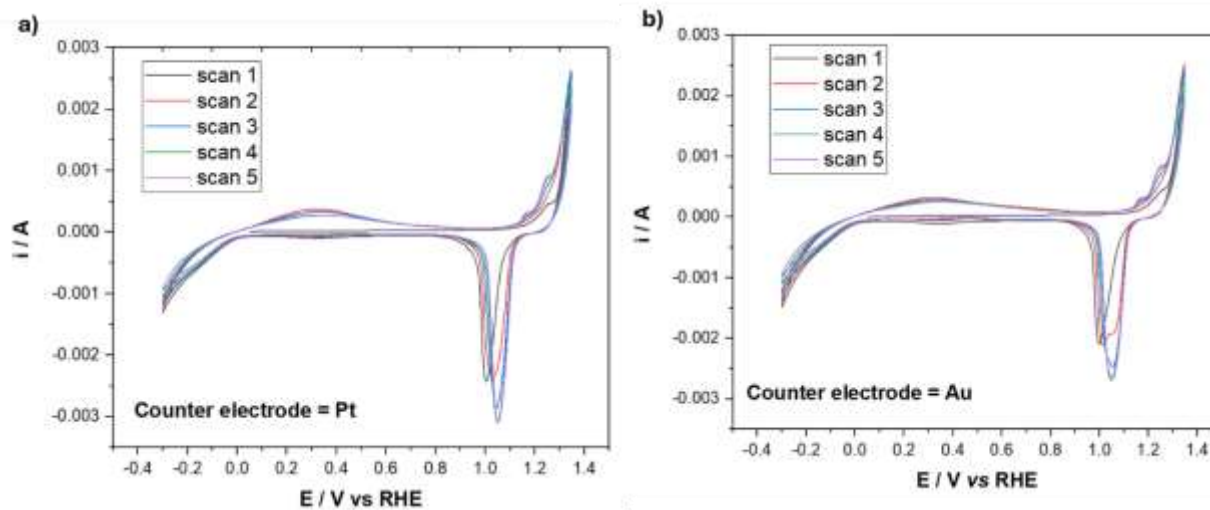


Figure S9: Cyclic voltammograms performed in NaOH 0.5 mol.L⁻¹ at 50 mV.s⁻¹ for Pt0.5Ag/C using a) Pt mesh and b) Au mesh as counter electrodes.

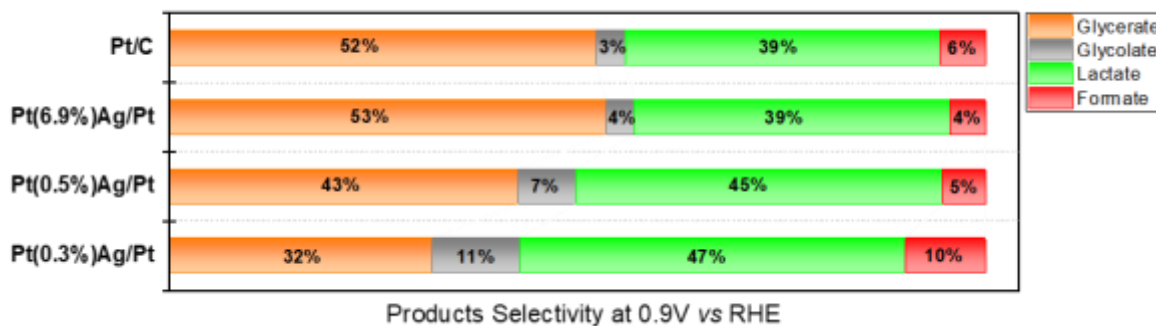


Figure S10: Products Selectivity at 0.9V vs RHE for GEOR on Pt/C, Pt(6.9%)Ag/C, Pt(0.5%)Ag/C, Pt(0.3%)Ag/C catalysts.

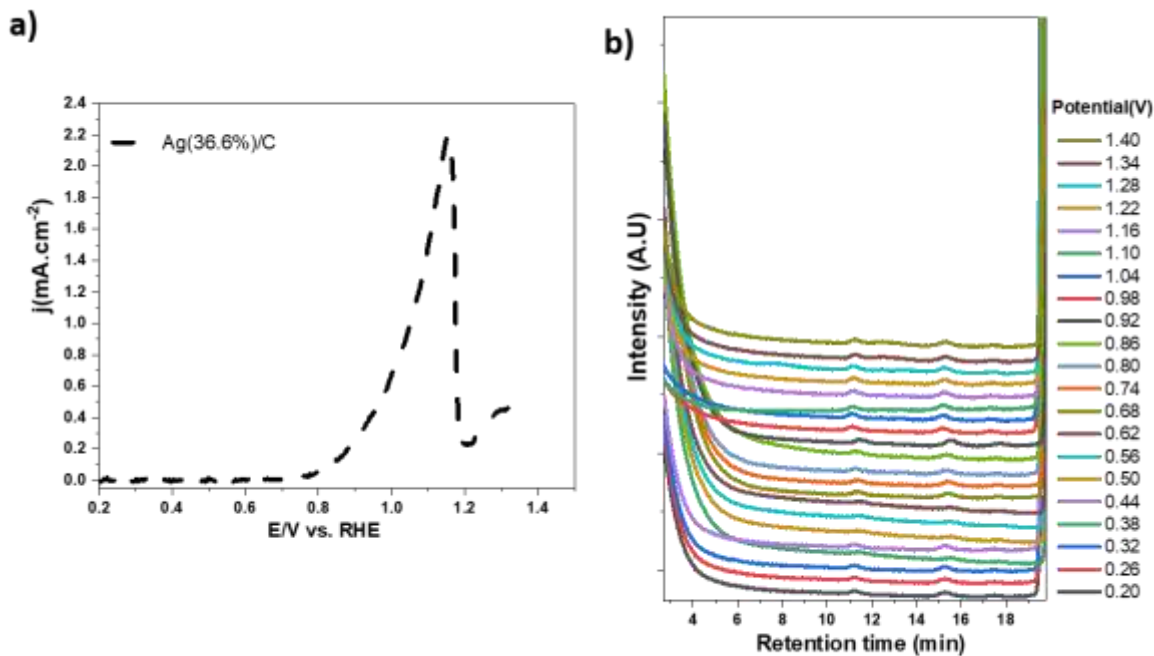


Figure S11: a) Linear Sweep Voltammetry of Ag/C catalyst recorded at 0.10 mV s⁻¹ in 1.0 M GIOH + 0.5 M NaOH. and the respective b) Chromatograms obtained during LSL from 0.2 – 1.35V range, scan rate 1.0 mVs⁻¹.

References

- (1) Shard, A. G. Practical Guides for X-Ray Photoelectron Spectroscopy: Quantitative XPS. *Journal of Vacuum Science & Technology A: Vacuum, Surfaces, and Films* **2020**, *38* (4), 1–13. <https://doi.org/10.1116/1.5141395>.
- (2) Xu, H.; Song, P.; Fernandez, C.; Wang, J.; Shiraishi, Y.; Wang, C.; Du, Y. Surface Plasmon Enhanced Ethylene Glycol Electrooxidation Based on Hollow Platinum-Silver Nanodendrites Structures. *J Taiwan Inst Chem Eng* **2018**, *91*, 316–322. <https://doi.org/10.1016/j.jtice.2018.05.036>.
- (3) Merkoçi, F.; Patarroyo, J.; Russo, L.; Piella, J.; Genç, A.; Arbiol, J.; Bastús, N. G.; Puntès, V. Understanding Galvanic Replacement Reactions: The Case of Pt and Ag. *Mater Today Adv* **2020**, *5*, 100037. <https://doi.org/10.1016/j.mtadv.2019.100037>.
- (4) Sharma, J.; DiBona, P.; Wiegand, D. A. XPS STUDIES OF THE PHOTODECOMPOSITION OF AgCl. **1982**, *12*, 420–424.
- (5) Sellin, R.; Clacens, J. M.; Coutanceau, C. A Thermogravimetric Analysis/Mass Spectroscopy Study of the Thermal and Chemical Stability of Carbon in the Pt/C Catalytic System. *Carbon NY* **2010**, *48* (8), 2244–2254. <https://doi.org/10.1016/j.carbon.2010.02.034>.
- (6) Santos, K. D. O.; Elias, W. C.; Signori, A. M.; Giacomelli, F. C.; Yang, H.; Domingos, J. B. Synthesis and Catalytic Properties of Silver Nanoparticle-Linear Polyethylene Imine Colloidal Systems. *Journal of Physical Chemistry C* **2012**, *116* (7), 4594–4604. https://doi.org/10.1021/JP2087169/SUPPL_FILE/JP2087169_SI_001.PDF.